Spatial metabolomics to profile metabolic reprogramming of liver in

Schistosoma japonicum-infected mice

Yu Zhang[†1,2,3], Ming Luo[†4], Junhui Li[1,2,3], Chen Guo[1,2,3], Jie Jiang[1,2,3], Ying Zhang[1,2,3], Gao Tan[5],

Xiaoli Liu[5] and Yingzi Ming[1,2,3]

[1] Transplantation Center, The Third Xiangya Hospital, Central South University, Changsha,

Hunan, China.

[2] NHC key laboratory of translational research on transplantation medicine, Changsha,

Hunan, China.

[3] Hunan Province Clinical Research Center for Infectious Diseases, Changsha, Hunan, China.

[4] Zhongnan Hospital of Wuhan University, Institute of Hepatobiliary Diseases of Wuhan

University, Transplant Center of Wuhan University, Wuhan, China.

[5] Hospital of the Hunan Provincial Corps of the People's Armed Police Force, Changsha,

Hunan, China.

†Yu Zhang and Ming Luo contributed equally to this work.

Corresponding author: Yingzi Ming. E-mail: 600941@csu.edu.cn

Abstract

Schistosomiasis is a parasitic disease that imposes a significant burden on society. The eggs are the primary pathogenic factor in schistosomiasis, and their accumulation in liver could lead to the formation of granulomas and liver fibrosis. However, the metabolic changes in liver resulting from schistosomiasis remain poorly understood. We established a mouse model of schistosomiasis japonica, where the eggs accumulate in the liver and form egg granulomas. We used mass spectrometry imaging to analyze the differences in metabolites among various liver regions, including the liver tissue from normal mice, the liver area outside the granulomas in schistosomiasis mice, and the granuloma region in schistosomiasis mice. There were significant differences in metabolites between different liver regions, which enriched in metabolic pathways such as the biosynthesis of unsaturated fatty acids, taurine and hypotaurine metabolism, glycerophospholipid metabolism, glycolysis/gluconeogenesis, purine metabolism, arachidonic acid metabolism, and bile secretion. In normal liver tissue, higher concentrations of oleic acid (FA (18:1)), eicosapentaenoic acid (FA (20:5)), and L-glutamine were observed. In liver regions outside the granulomas, D-glucose and pyruvic acid were elevated compared to those in normal mice. Taurine increased in the liver of schistosomiasis. Meanwhile, there were elevated uric acid and spermidine in the egg granulomas. We employed MSI technology to investigate metabolic reprogramming in liver of *S. japonicum*-infected mice. We explored the spatial distribution of differential metabolites in liver of schistosomiasis including unsaturated fatty acids, taurine, glutamine, spermidine, and uric acid. Our research provides valuable insights for further elucidating metabolic reprogramming in schistosomiasis.

Keywords: Schistosomiasis, Spatial metabolomics, Mass Spectrometry Imaging

Introduction

Schistosomiasis is a neglected tropical disease that imposes a significant burden on society, affecting over 200 million people worldwide (McManus *et al*., 2018). The schistosomes that infect humans include three main species: *Schistosoma haematobium* (*S. haematobium*), *S. mansoni,* and *S. japonicum* (Wang *et al*., 2013). Acute schistosomiasis occurs when humans contact with water containing cercariae. Inside the host, cercariae develop into adult worms , which then produce eggs deposited in tissues (Ross *et al*., 2007). Praziquantel is an effective treatment for schistosomiasis, but it primarily kills adult worms and is less effective against eggs. Eggs are a major pathogenic factor in chronic schistosomiasis (Colley *et al*., 2014). S. *haematobium* mainly affects the urinary system, while *S. mansoni* and *S. japonicum* primarily affect the mesenteric venous system (Zhang *et al*., 2007). Eggs deposited in the liver attract various immune cells, leading to the formation of egg granulomas and promoting liver fibrosis (Chuah *et al*., 2014). Schistosoma-associated liver fibrosis could cause portal hypertension, resulting in splenomegaly, ascites, and esophageal and gastric varices, which are significant factors contributing to the poor prognosis of patients with schistosomiasis (Li *et al*., 2019).

The liver is a crucial organ for metabolism, acting as a major hub for energy synthesis and conversion. Liver maintains blood sugar levels by regulating the synthesis and breakdown of glucose (Han *et al*., 2016). Additionally, the liver plays a vital role in lipid metabolism, overseeing the synthesis and degradation of fatty acids as well as the production and transport of cholesterol (Badmus *et al*., 2022). It synthesizes essential plasma proteins, including albumin, clotting factors, and transport proteins, and liver is also involved in amino

acid metabolism by converting ammonia into urea for excretion through the urea cycle (Paulusma *et al*., 2022). Schistosomiasis could affect the glucose and lipid metabolism (Cai *et al*., 2021). Clinical results have showed that the serum levels of total cholesterol (TC), triglycerides (TG), and HDL-C in the infected individuals with schistosomiasis were lower than those in the uninfected group, which indicate a lower risk of developing atherosclerosis (Shen *et al*., 2015; Zinsou *et al*., 2020). Additionally, host insulin sensitivity increases in schistosomiasis, with upregulation of glycolysis-related gene expression and downregulation of gluconeogenesis gene expression (Xu *et al*., 2019). The deposition of eggs in the liver causes granuloma formation and liver fibrosis, and the impact of these changes on liver metabolism requires further investigation.

Metabolites are small molecules generated during metabolic processes within organisms. These include carbohydrates, lipids, amino acids, and nucleotides, all of which are essential for cellular physiological and biochemical functions (Husted *et al*., 2017). Liquid chromatography-mass spectrometry (LC-MS) has become the predominant analytical technique in metabolomics research, offering insights into thousands of metabolites in a single analysis. It is particularly valuable for metabolomic analyses of biological samples such as blood, urine, and cells (Chen *et al*., 2023). However, LC-MS methods have limitations when analyzing metabolites in complex and heterogeneous tissues or organs. During the tissue homogenization, metabolite extraction, purification, and enrichment, it results in the loss of spatial distribution information of metabolites within the tissues. Mass Spectrometry Imaging (MSI) is an advanced molecular imaging technique that directly provides detailed structural, quantitative, and spatial distribution information of metabolites

(Unsihuay *et al.*, 2021). In this study, we employed MSI to explore the metabolic reprogramming of liver in *S. japonicum*-infected mice.

Methods

Mice model of Schistosomiasis japonica

Male C57BL/6 mice, 6 weeks old, were purchased from Hunan Slack Jingda Experimental Animal Company. At the Experimental Animal Center of Central South University, the mice were housed under specific pathogen-free conditions and free access to food and water. The protocols for the animal experiments were approved by the local ethics committee for The Third Xiangya Hospital of Central South University (Changsha, China). *S. japonicum*-infected Oncomelania hupensis snails were supplied by Hunan Provincial Institute of Parasitic Diseases in China. Following the induction of cercarial release, the mice were infected percutaneously with fresh cercariae (25±2). On day 35 post-infection, the mice were administered praziquantel (500 mg/kg, once daily for 2 days). The mice were sacrificed until week 8 after infection.

Sample preparation

Fresh liver tissue from *S. japonicum*-infected mouse (n=1) and normal mouse (n=1) was embedded and then sectioned into approximately 10 μm thick slices using a cryostat microtome (Leica CM 1950, Leica Microsystem, Germany). The sections were thaw-mounted on positive charge desorption plate (Thermo Scientific, U.S.A) and stored at -80°C until needed. Prior to mass spectrometry imaging (MSI) analysis, the slices were

desiccated at -20°C for 1 hour and then at room temperature for 2 hours before being analyzed. Additionally, a neighboring section was reserved for hematoxylin-eosin (H&E) staining.

Data acquisition and MSI analysis

MSI analysis was conducted following the methods described by Luo *et al* (Luo *et al*., 2013). The experiment was performed using an AFADESI-MSI platform (Beijing Victor Technology Co., LTD, Beijing, China) in tandem with a Q-Orbitrap mass spectrometer (Q Exactive, Thermo Scientific, U.S.A.). For negative ion mode, the spray solvent was acetonitrile (ACN)/H2O (8:2), and for positive ion mode, the spray solvent was ACN/H2O (8:2, 0.1% FA). The solvent flow rate was set at 5 μL/min, the transfer gas flow rate at 45 L/min, and the spray voltage at 7 kV. The distances between the sample surface and the sprayer, as well as between the sprayer and the ion transfer tube, were maintained at 3 mm. The MS resolution was set to 70,000, with a mass range of 70-1000 Da. The automated gain control (AGC) target was set to 2E6, with a maximum injection time of 200 ms. The S-lens voltage was set to 55 V, and the capillary temperature to 350°C. During MSI scanning, the speed in the X direction was 0.2 mm/s, and the vertical step size in the Y direction was 100 μm.

Data processing

The raw mass spectrometry files in .raw format were converted to .imzML format using imzMLConverter, and then imported into MSiReader (an open-source interface to view and analyze high resolving power MS imaging files on Matlab platform) (Race *et al*., 2012). Ion

images were reconstructed following background subtraction using the Cardinal software package (Bemis *et al*., 2015). All MS images were normalized using total ion count normalization (TIC) for each pixel (Wang *et al*., 2022). To precisely extract region-specific MS profiles, high spatial resolution H&E images were used for matching. Differences in metabolites across various tissue microregions were initially screened using supervised statistical analysis methods, specifically orthogonal partial least squares discrimination analysis (OPLS-DA). The variable importance of projection (VIP) values derived from the OPLS-DA model were used to describe the overall contribution of each metabolite to group differentiation. Metabolites with VIP values greater than 1 were considered potential differentiating metabolites. Subsequently, a two-tailed Student's T-test was employed to verify whether the differences in metabolites between groups were significant. Finally, metabolites with VIP values greater than 1.0 and P-values less than 0.05 were selected as differentiating metabolites.

Analyte Identification

The ions detected by AFADESI were annotated by the pySM pipeline and an in-house SmetDB database (Lumingbio, Shanghai, China) (Palmer *et al*., 2017).

Results

Spatial multivariate analysis of liver in S. japonicum-*infected mice*

We constructed *S. japonicum*-induced mice, and the eggs deposited in livers were surrounded by a large number of immune cells, forming egg granulomas (Fig. 1A). The liver tissue can

be categorized into the following regions: (A) the liver tissue from normal mice, (B) the liver area outside the granulomas in mice of schistosomiasis, (C) the granuloma region in mice of schistosomiasis. To investigate the metabolic changes of liver in schistosomiasis, we conducted MSI analysis on the livers of both normal and Schistosoma-infected mice. The mass spectrometry spectra revealed the intensity of the mass-to-charge ratios (m/z) for livers of Schistosoma-infected mice and normal mice negative and positive ion modes (Fig. 1B). These spectra were generated by averaging the m/z intensity across each pixel. We employed multivariate statistical analysis to compare the different regions. In both negative and positive ion modes, there were significant differences in metabolic distribution between the normal liver area (Area A) and the liver area outside the granulomas (Area B), as well as between the normal liver area (Area A) and the granuloma region (Area C) (Fig. 1C). We evaluated the quality of the model using 200 rounds of response permutation testing (RPT). The Q2 values for all group comparisons were less than zero, indicating that the OPLS-DA model was not overfitted (Fig. 1D).

Differential metabolites in the liver of schistosomiasis

We identified differential metabolites across different regions. Compared to Area B, Area A exhibited 215 downregulated and 149 upregulated metabolites in the negative ion mode, and 127 downregulated and 303 upregulated metabolites in the positive ion mode (Fig. 2A). In the OPLS-DA analysis, we used variable importance in projection (VIP) values to assess the influence and explanatory power of each metabolite's expression pattern on sample classification. To identify biologically significant differential metabolites, we combined

multivariate and univariate analyses. We selected metabolites with VIP values greater than 1 in the PLS-DA model and a p-value less than 0.05 in the t-test. Based on this, the analysis in the negative ion mode revealed 34 downregulated and 22 upregulated differential metabolites, while in the positive ion mode, there were 46 upregulated and 27 downregulated differential metabolites (Fig. 2B). When comparing area A with area C, we found 223 downregulated and 224 upregulated differential metabolites in the negative ion mode, and 323 upregulated and 138 downregulated in the positive ion mode (Fig. 2C). Among these metabolites with VIP values >1 included 20 downregulated and 28 upregulated in the negative ion mode, and 55 upregulated and 28 downregulated in the positive ion mode (Fig. 2D).

Functional enrichment analysis of differential metabolites

We integrated differential metabolites with VIP values >1 and p-values <0.05 from the t-test, including those identified in both the negative and positive ion modes. To further understand the functions of these differential metabolites, we performed KEGG functional enrichment analysis. Compared to area A, the functional enrichment of differential metabolites in area B was associated with linoleic acid metabolism, biosynthesis of unsaturated fatty acids, taurine and hypotaurine metabolism, glycerophospholipid metabolism, glycolysis/gluconeogenesis, purine metabolism, and primary bile acid biosynthesis (Fig. 3A). When comparing area A with area C, the functional enrichment of differential metabolites was linked to arachidonic acid metabolism, biosynthesis of unsaturated fatty acids, arginine and proline metabolism, taurine and hypotaurine metabolism, and bile secretion (Fig. 3B).

In situ distribution of crucial differential metabolites in the liver of schistosomiasis

Unsaturated fatty acids, including FA (18:1), FA (18:2), FA (18:3), FA (20:1), FA (20:3), FA (20:4), FA (20:5), FA (22:4), and FA (22:6), exhibited significant differences across various liver regions. In normal liver (Area A), FA (18:1) and FA (20:5) were abundant. In the liver area outside the granulomas (Area B), FA (18:2) and FA (18:3) were predominant. In the granuloma region (Area C), the primary unsaturated fatty acids were FA (20:4) and FA (22:4) (Fig. 4). Phospholipids have multiple functions, including maintaining the normal structure and function of biological membranes, participating in cell signaling, and facilitating the absorption and transport of fats and fat-soluble substances. In normal liver tissue (Area A), PE (36:4) and LPC (22:6) were present in high levels, while PC (32:0) was predominantly found in the granuloma region (Area C) (Fig. 5A). In the liver area outside the granulomas (Area B), the levels of D-glucose, gluconic acid, and pyruvic acid were elevated (Fig. 5B). Taurine were notably higher in the liver of schistosomiasis (Area B and Area C), while L-glutamine was increased in normal liver (Area A). Spermidine levels was abundant in the granuloma region (Area C) (Fig. 5C). Additionally, there were differences in purine metabolism. Hypoxanthine was higher in normal liver (Area A), whereas xanthine was elevated in the liver of schistosomiasis (Area B and Area C), and uric acid was increased around the granuloma region (Area C) (Fig. 5D).

Discussion

Schistosomiasis is a parasitic disease that triggers immune responses and inflammatory changes, while also impacting the metabolism of host. Traditional LC-MS techniques are

widely employed for metabolite analysis; however, they analyze whole tissues and lack spatial resolution. Schistosome eggs deposited in the liver lead to the formation of granulomas and liver fibrosis. In schistosomiasis, there are notable metabolic differences between granuloma regions and the surrounding liver tissue. To better detect and understand the progression of schistosomiasis, we employed MSI to investigate the metabolism in the liver of schistosomiasis.

We conducted a comparative analysis of the liver in normal mice (Area A), the liver areas outside granulomas in schistosomiasis (Area B), and the granuloma regions in schistosomiasis (Area C). Significant differences were observed in the metabolites among these regions. The pathways enriched with differential metabolites were primarily associated with the biosynthesis of unsaturated fatty acids, taurine and hypotaurine metabolism, glycerophospholipid metabolism, glycolysis/gluconeogenesis, purine metabolism, primary bile acid biosynthesis, arachidonic acid metabolism, and bile secretion. Studies showed that genes involved in metabolic processes within hepatic granulomas, compared to uninfected controls, were associated with the metabolism of xenobiotics, sterols, fatty acids, and vitamin (Chuah *et al*., 2013). In our research, there were significant differences in the abundance of unsaturated fatty acids among the three regions. In normal liver tissue (Area A), oleic acid (FA (18:1)) and eicosapentaenoic acid (FA (20:5)) were present in higher concentrations. Some research show that oleic acid has anti-apoptotic effects and helps alleviate endoplasmic reticulum (ER) stress, playing a crucial protective role in liver cells (Liu *et al*., 2023). The levels of oleic acid were reduced in liver of schistosomiasis, indicating that liver cells might be more vulnerable to damage in schistosomiasis. Current research also shows that

eicosapentaenoic acid could inhibit lipogenesis and promote liver fatty acid oxidation (Sugiyama *et al*., 2008). In the liver of schistosomiasis, linoleic acid (FA (18:2)) and α-linolenic acid (FA (18:3)) were more highly expressed in the liver regions outside the granulomas (Area B). Linoleic acid and α-linolenic acid are classified as polyunsaturated omega-6 and omega-3 fatty acids, respectively. Linoleic acid and its oxidized metabolites might exacerbate liver damage by promoting inflammatory responses, and the accumulation of linoleic acid in liver of schistosomiasis could be a potential cause of liver damage (Warner *et al*., 2017). In contrast, α-linolenic acid has different effects; it could improve insulin resistance and reduce inflammatory responses (Gonçalves *et al*., 2018). In the granuloma regions, the unsaturated fatty acids identified included arachidonic acid (FA (20:4)) and FA (22:4), both of which are polyunsaturated omega-6 fatty acids. The deposition of eggs in the liver leads to significant immune cell infiltration, and arachidonic acid, as an inflammatory mediator, might play a crucial role in driving the inflammatory response (Sonnweber *et al*., 2018). Additionally, research has suggested that arachidonic acid could activate neutrophil sphingomyelinase bound to the surface of Schistosoma, which then hydrolyzes sphingomyelin molecules in the lipid bilayer, potentially offering an effective treatment strategy for schistosomiasis (El Ridi *et al*., 2010; El Ridi and Tallima 2013; Tallima *et al*., 2020). However, current research primarily focuses on *Schistosoma* larvae and adults, and whether arachidonic acid is effective against eggs still requires further investigation.

Phospholipids have multiple functions, including maintaining the normal structure and function of biological membranes, participating in cell signaling, and facilitating the absorption and transport of fats and fat-soluble fibers (Ecker and Liebisch 2014). In normal

liver tissue, PE (36:4) levels were relatively high, whereas PC (32:0) was more prevalent in granuloma regions. Alterations in lipid composition might influence the functionality of membrane proteins, including receptors, ion channels, and transporters. Research has shown that schistosomiasis affected the glucose metabolism of host, leading to the upregulation of glycolysis-related genes in the liver, such as *Ldha*, *Glut4*, *Pkm2*, *Glut1*, *Pfkfb3*, *Aldoc*, *HK2*, and *Pfk*, and could also improve insulin resistance (Cai *et al*., 2021; Xu *et al*., 2019). Our results indicated that in liver regions outside the granulomas, levels of D-glucose and pyruvic acid were higher compared to those in normal mice, suggesting increased glucose metabolism. This might be due to a compensatory enhancement of glucose metabolism in the remaining liver cells, associated with granuloma formation and liver cell damage. Meanwhile, our results showed that taurine was increased in liver of schistosomiasis (Area B an Area C). Taurine is a versatile amino acid that aids in bile production and secretion, while its antioxidant properties help neutralize free radicals and reduce oxidative stress damage to cells (McGaunn and Baur 2023). Taurine has also been shown to improve liver granulomas and fibrosis in mice with schistosomiasis (Yu *et al*., 2016). Additionally, elevated Taurine might serve as a potential diagnostic marker for schistosomiasis (Wang *et al*., 2004). L-glutamine levels were reduced in the liver of schistosomiasis. Glutamine is one of the most abundant and versatile amino acids in the body, essential for maintaining cellular energy metabolism, nucleotide and amino acid biosynthesis, and redox balance (Vander Heiden *et al*., 2009). Additionally, it is crucial for lymphocyte proliferation, cytokine production, macrophage activation, and neutrophil bactericidal activity (Cruzat *et al*., 2018). During the formation of egg granulomas and liver fibrosis, the active inflammatory response of immune cells might

lead to increased consumption of glutamine. Meanwhile, high levels of spermidine were observed in the liver of schistosomiasis. Spermidine plays a crucial role in regulating immune cells (Chamoto *et al*., 2024). It promotes a shift in macrophages towards an anti-inflammatory phenotype, which helps to reduce inflammation (Yang *et al*., 2016). Additionally, spermidine is essential for the differentiation of T cells, B cells, and natural killer (NK) cells, and it helps maintain their functional stability (O'Brien *et al*., 2021; Puleston *et al*., 2014; Zhang *et al*., 2019). Elevated spermidine levels might play a significant role in sustaining the function of immune cells in egg granulomas. Our results revealed elevated uric acid levels in the egg granulomas. Hypoxanthine is metabolized by xanthine dehydrogenase into xanthine, which is then further converted into uric acid. As the final product of purine metabolism, uric acid can accumulate excessively, leading to inflammatory arthritis and gout. However, research suggests that uric acid might also promote Th2 cell immunity by activating dendritic cells through spleen tyrosine kinase and PI3-kinase δ signaling pathway (Kool *et al*., 2011). Schistosomiasis is closely associated with type 2 immunity, with Th2 cells facilitating granuloma formation and liver fibrosis (Fairfax *et al*., 2012). Uric acid exhibits potential in promoting type 2 immunity, though its mechanisms require further investigation.

Conclusions

Our study primarily explored the metabolic reprogramming of the liver in schistosomiasis through spatial localization. The differential metabolites across different liver regions were associated with pathways including the biosynthesis of unsaturated fatty acids, taurine and

hypotaurine metabolism, glycerophospholipid metabolism, glycolysis/gluconeogenesis, purine metabolism, primary bile acid biosynthesis, arachidonic acid metabolism, and bile secretion. We observed many differential metabolites, such as unsaturated fatty acids, taurine, glutamine, spermidine, and uric acid, and their spatial distribution in the liver of schistosomiasis. We also hope that the spatial distribution of differential metabolites will provide valuable insights for understanding the pathogenesis and progression of schistosomiasis.

Competing interests. The authors declare that they have no conflict of interest.

Ethical standards. Our study was approved by the Ethics Committee of the 3rd Xiangya Hospital of Central South University (Ethics Review No. 21145). This study does not involve patients' informed consent.

Author contributions. YZ, ML, and YM contributed to the study design. CG, JJ, JL, and YZ contributed to the collection of samples. YZ, ML, GT and JL contributed to collect and

analyze data. YZ, ML, XL and YM contributed to the manuscript development. All authors provided critical revisions and took responsibility for the work. All the authors have read and approved the final manuscript.

Availability of data and materials. All of data and materials are available.

References

Badmus OO, Hillhouse SA, Anderson CD, Hinds TD and Stec DE (2022) Molecular mechanisms of metabolic associated fatty liver disease (MAFLD): functional analysis of lipid metabolism pathways. *Clin Sci (Lond)* **136** (18)**,** 1347-1366. https://doi.org/10.1042/cs20220572.

Bemis KD, Harry A, Eberlin LS, Ferreira C, van de Ven SM, Mallick P, Stolowitz M and Vitek O (2015) Cardinal: an R package for statistical analysis of mass spectrometry-based imaging experiments. *Bioinformatics* **31** (14)**,** 2418-2420. https://doi.org/10.1093/bioinformatics/btv146.

Cai Z, Deng X, Zhao L, Wang X, Yang L and Yuan G (2021) The relationship between Schistosoma and glycolipid metabolism. *Microb Pathog* **159,** 105120. https://doi.org/10.1016/j.micpath.2021.105120.

Chamoto K, Zhang B, Tajima M, Honjo T and Fagarasan S (2024) Spermidine - an old molecule with a new age-defying immune function. *Trends Cell Biol* **34** (5)**,** 363-370. https://doi.org/10.1016/j.tcb.2023.08.002.

Chen CJ, Lee DY, Yu J, Lin YN and Lin TM (2023) Recent advances in LC-MS-based metabolomics for clinical biomarker discovery. *Mass Spectrom Rev* **42** (6)**,** 2349-2378. https://doi.org/10.1002/mas.21785.

Chuah C, Jones MK, Burke ML, McManus DP and Gobert GN (2014) Cellular and chemokine-mediated regulation in schistosome-induced hepatic pathology. *Trends Parasitol* **30** (3)**,** 141-150. https://doi.org/10.1016/j.pt.2013.12.009.

Chuah C, Jones MK, Burke ML, Owen HC, Anthony BJ, McManus DP, Ramm GA and

Gobert GN (2013) Spatial and temporal transcriptomics of Schistosoma japonicum-induced hepatic granuloma formation reveals novel roles for neutrophils. *J Leukoc Biol* **94** (2)**,** 353-365. https://doi.org/10.1189/jlb.1212653.

Colley DG, Bustinduy AL, Secor WE and King CH (2014) Human schistosomiasis. *Lancet* **383** (9936)**,** 2253-2264. https://doi.org/10.1016/s0140-6736 (13)61949-2.

Cruzat V, Macedo Rogero M, Noel Keane K, Curi R and Newsholme P (2018) Glutamine: Metabolism and Immune Function, Supplementation and Clinical Translation. *Nutrients* **10** (11). https://doi.org/10.3390/nu10111564.

Ecker J and Liebisch G (2014) Application of stable isotopes to investigate the metabolism of fatty acids, glycerophospholipid and sphingolipid species. *Prog Lipid Res* **54,** 14-31. https://doi.org/10.1016/j.plipres.2014.01.002.

El Ridi R, Aboueldahab M, Tallima H, Salah M, Mahana N, Fawzi S, Mohamed SH and Fahmy OM (2010) In vitro and in vivo activities of arachidonic acid against Schistosoma mansoni and Schistosoma haematobium. *Antimicrob Agents Chemother* **54** (8)**,** 3383-3389. https://doi.org/10.1128/aac.00173-10.

El Ridi RA and Tallima HA (2013) Novel therapeutic and prevention approaches for schistosomiasis: review. *J Adv Res* **4** (5)**,** 467-478. https://doi.org/10.1016/j.jare.2012.05.002.

Fairfax K, Nascimento M, Huang SC, Everts B and Pearce EJ (2012) Th2 responses in schistosomiasis. *Semin Immunopathol* **34** (6)**,** 863-871. https://doi.org/10.1007/s00281-012-0354-4.

Gonçalves NB, Bannitz RF, Silva BR, Becari DD, Poloni C, Gomes PM, Foss MC and

Foss-Freitas MC (2018) α-Linolenic acid prevents hepatic steatosis and improves glucose tolerance in mice fed a high-fat diet. *Clinics (Sao Paulo)* **73,** e150. https://doi.org/10.6061/clinics/2018/e150.

Han HS, Kang G, Kim JS, Choi BH and Koo SH (2016) Regulation of glucose metabolism from a liver-centric perspective. *Exp Mol Med* **48** (3)**,** e218. https://doi.org/10.1038/emm.2015.122.

Husted AS, Trauelsen M, Rudenko O, Hjorth SA and Schwartz TW (2017) GPCR-Mediated Signaling of Metabolites. *Cell Metab* **25** (4)**,** 777-796. https://doi.org/10.1016/j.cmet.2017.03.008.

Kool M, Willart MA, van Nimwegen M, Bergen I, Pouliot P, Virchow JC, Rogers N, Osorio F, Reis e Sousa C, Hammad H and Lambrecht BN (2011) An unexpected role for uric acid as an inducer of T helper 2 cell immunity to inhaled antigens and inflammatory mediator of allergic asthma. *Immunity* **34** (4)**,** 527-540. https://doi.org/10.1016/j.immuni.2011.03.015.

Li G, Huang S, Lian L, Song X, Sun W, Miao J, Li B, Yuan Y, Wu S, Liu X and Zhu Z (2019) Derivation and external validation of a model to predict 2-year mortality risk of patients with advanced schistosomiasis after discharge. *EBioMedicine* **47,** 309-318. https://doi.org/10.1016/j.ebiom.2019.08.028.

Liu W, Zhu M, Gong M, Zheng W, Zeng X, Zheng Q, Li X, Fu F, Chen Y, Cheng J, Rao Z, Lu Y and Chen Y (2023) Comparison of the Effects of Monounsaturated Fatty Acids and Polyunsaturated Fatty Acids on Liver Lipid Disorders in Obese Mice. *Nutrients* **15** (14). https://doi.org/10.3390/nu15143200.

Luo Z, He J, Chen Y, He J, Gong T, Tang F, Wang X, Zhang R, Huang L, Zhang L, Lv H, Ma S, Fu Z, Chen X, Yu S and Abliz Z (2013) Air flow-assisted ionization imaging mass spectrometry method for easy whole-body molecular imaging under ambient conditions. *Anal Chem* **85** (5)**,** 2977-2982. https://doi.org/10.1021/ac400009s.

McGaunn J and Baur JA (2023) Taurine linked with healthy aging. *Science* **380** (6649)**,** 1010-1011. https://doi.org/10.1126/science.adi3025.

McManus DP, Dunne DW, Sacko M, Utzinger J, Vennervald BJ and Zhou XN (2018) Schistosomiasis. *Nat Rev Dis Primers* **4** (1)**,** 13. https://doi.org/10.1038/s41572-018-0013-8.

O'Brien KL, Assmann N, O'Connor E, Keane C, Walls J, Choi C, Oefner PJ, Gardiner CM, Dettmer K and Finlay DK (2021) De novo polyamine synthesis supports metabolic and functional responses in activated murine NK cells. *Eur J Immunol* **51** (1)**,** 91-102. https://doi.org/10.1002/eji.202048784.

Palmer A, Phapale P, Chernyavsky I, Lavigne R, Fay D, Tarasov A, Kovalev V, Fuchser J, Nikolenko S, Pineau C, Becker M and Alexandrov T (2017) FDR-controlled metabolite annotation for high-resolution imaging mass spectrometry. *Nat Methods* **14** (1)**,** 57-60. https://doi.org/10.1038/nmeth.4072.

Paulusma CC, Lamers WH, Broer S and van de Graaf SFJ (2022) Amino acid metabolism, transport and signalling in the liver revisited. *Biochem Pharmacol* **201,** 115074. https://doi.org/10.1016/j.bcp.2022.115074.

Puleston DJ, Zhang H, Powell TJ, Lipina E, Sims S, Panse I, Watson AS, Cerundolo V, Townsend AR, Klenerman P and Simon AK (2014) Autophagy is a critical regulator of

memory CD8 (+) T cell formation. *Elife* **3**. https://doi.org/10.7554/eLife.03706.

Race AM, Styles IB and Bunch J (2012) Inclusive sharing of mass spectrometry imaging data requires a converter for all. *J Proteomics* **75** (16)**,** 5111-5112. https://doi.org/10.1016/j.jprot.2012.05.035.

Ross AG, Vickers D, Olds GR, Shah SM and McManus DP (2007) Katayama syndrome. *Lancet Infect Dis* **7** (3)**,** 218-224. https://doi.org/10.1016/s1473-3099 (07)70053-1.

Shen SW, Lu Y, Li F, Shen ZH, Xu M, Yao WF, Feng YB, Yun JT, Wang YP, Ling W, Qi HJ and Tong DX (2015) Potential long-term effects of previous schistosome infection may reduce the atherogenic index of plasma in Chinese men. *Int J Parasitol* **45** (5)**,** 289-294. https://doi.org/10.1016/j.ijpara.2015.01.001.

Sonnweber T, Pizzini A, Nairz M, Weiss G and Tancevski I (2018) Arachidonic Acid Metabolites in Cardiovascular and Metabolic Diseases. *Int J Mol Sci* **19** (11). https://doi.org/10.3390/ijms19113285.

Sugiyama E, Ishikawa Y, Li Y, Kagai T, Nobayashi M, Tanaka N, Kamijo Y, Yokoyama S, Hara A and Aoyama T (2008) Eicosapentaenoic acid lowers plasma and liver cholesterol levels in the presence of peroxisome proliferators-activated receptor alpha. *Life Sci* **83** (1-2)**,** 19-28. https://doi.org/10.1016/j.lfs.2008.04.011.

Tallima H, Hanna VS and El Ridi R (2020) Arachidonic Acid Is a Safe and Efficacious Schistosomicide, and an Endoschistosomicide in Natural and Experimental Infections, and Cysteine Peptidase Vaccinated Hosts. *Front Immunol* **11,** 609994. https://doi.org/10.3389/fimmu.2020.609994.

Unsihuay D, Mesa Sanchez D and Laskin J (2021) Quantitative Mass Spectrometry

Imaging of Biological Systems. *Annu Rev Phys Chem* **72,** 307-329. https://doi.org/10.1146/annurev-physchem-061020-053416.

Vander Heiden MG, Cantley LC and Thompson CB (2009) Understanding the Warburg effect: the metabolic requirements of cell proliferation. *Science* **324** (5930)**,** 1029-1033. https://doi.org/10.1126/science.1160809.

Wang G, Heijs B, Kostidis S, Mahfouz A, Rietjens RGJ, Bijkerk R, Koudijs A, van der Pluijm LAK, van den Berg CW, Dumas SJ, Carmeliet P, Giera M, van den Berg BM and Rabelink TJ (2022) Analyzing cell-type-specific dynamics of metabolism in kidney repair. *Nat Metab* **4** (9)**,** 1109-1118. https://doi.org/10.1038/s42255-022-00615-8.

Wang WL, Song LJ, Chen X, Yin XR, Fan WH, Wang GP, Yu CX and Feng B (2013) Synthesis and SAR studies of praziquantel derivatives with activity against Schistosoma japonicum. *Molecules* **18** (8)**,** 9163-9178. https://doi.org/10.3390/molecules18089163.

Wang Y, Holmes E, Nicholson JK, Cloarec O, Chollet J, Tanner M, Singer BH and Utzinger J (2004) Metabonomic investigations in mice infected with Schistosoma mansoni: an approach for biomarker identification. *Proc Natl Acad Sci U S A* **101** (34)**,** 12676-12681. https://doi.org/10.1073/pnas.0404878101.

Warner DR, Liu H, Miller ME, Ramsden CE, Gao B, Feldstein AE, Schuster S, McClain CJ and Kirpich IA (2017) Dietary Linoleic Acid and Its Oxidized Metabolites Exacerbate Liver Injury Caused by Ethanol via Induction of Hepatic Proinflammatory Response in Mice. *Am J Pathol* **187** (10)**,** 2232-2245. https://doi.org/10.1016/j.ajpath.2017.06.008.

Xu ZP, Chang H, Ni YY, Li C, Chen L, Hou M and Ji MJ (2019) Schistosoma japonicum

infection causes a reprogramming of glycolipid metabolism in the liver. *Parasit Vectors* **12** (1)**,** 388. https://doi.org/10.1186/s13071-019-3621-6.

Yang Q, Zheng C, Cao J, Cao G, Shou P, Lin L, Velletri T, Jiang M, Chen Q, Han Y, Li F, Wang Y, Cao W and Shi Y (2016) Spermidine alleviates experimental autoimmune encephalomyelitis through inducing inhibitory macrophages. *Cell Death Differ* **23** (11)**,** 1850-1861. https://doi.org/10.1038/cdd.2016.71.

Yu YR, Ni XQ, Huang J, Zhu YH and Qi YF (2016) Taurine drinking ameliorates hepatic granuloma and fibrosis in mice infected with Schistosoma japonicum. *Int J Parasitol Drugs Drug Resist* **6** (1)**,** 35-43. https://doi.org/10.1016/j.ijpddr.2016.01.003.

Zhang H, Alsaleh G, Feltham J, Sun Y, Napolitano G, Riffelmacher T, Charles P, Frau L, Hublitz P, Yu Z, Mohammed S, Ballabio A, Balabanov S, Mellor J and Simon AK (2019) Polyamines Control eIF5A Hypusination, TFEB Translation, and Autophagy to Reverse B Cell Senescence. *Mol Cell* **76** (1)**,** 110-125.e119. https://doi.org/10.1016/j.molcel.2019.08.005.

Zhang Y, Koukounari A, Kabatereine N, Fleming F, Kazibwe F, Tukahebwa E, Stothard JR, Webster JP and Fenwick A (2007) Parasitological impact of 2-year preventive chemotherapy on schistosomiasis and soil-transmitted helminthiasis in Uganda. *BMC Med* **5,** 27. https://doi.org/10.1186/1741-7015-5-27.

Zinsou JF, Janse JJ, Honpkehedji YY, Dejon-Agobé JC, García-Tardón N, Hoekstra PT, Massinga-Loembe M, Corstjens P, van Dam GJ, Giera M, Kremsner PG, Yazdanbakhsh M, Adegnika AA and Guigas B (2020) Schistosoma haematobium infection is associated with lower serum cholesterol levels and improved lipid profile in

overweight/obese individuals. *PLoS Negl Trop Dis* **14** (7)**,** e0008464. https://doi.org/10.1371/journal.pntd.0008464.

Figure legends

Figure 1. Spatial multivariate analysis of liver in *S. japonicum*-infected mice. (A) HE staining of the liver of normal mouse and mouse with schistosomiasis. (B) Mass spectrometry of the liver of normal mouse and mouse with schistosomiasis under negative and positive ion modes. (C) OPLS-DA model analysis between Area A and Area B, as well as between Area A and Area C, under negative and positive ion modes. (D) Assessment of OPLS-DA model using 200 rounds of response permutation testing (RPT). (NC: normal control mouse; SJ: *S. japonicum*-infected mice; neg: negative ion modes; pos: positive ion modes; OPLS-DA: Orthogonal Partial Least Squares Discriminant Analysis; A: the liver tissue from normal mice (Area A); B: the liver area outside the granulomas in mice of schistosomiasis (Area B); C: the granuloma region in mice of schistosomiasis (Area C))
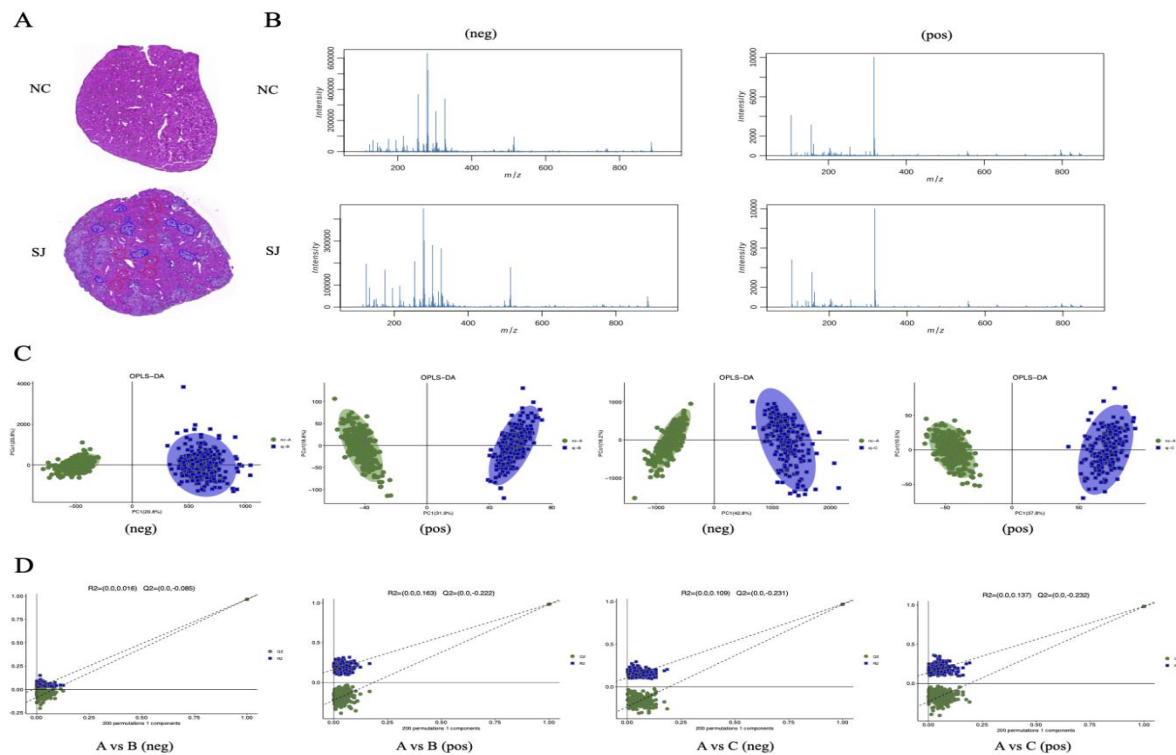
Figure 2. Differential metabolites in the liver of schistosomiasis. (A) Volcano plots of differential metabolites between Area A and Area B under negative and positive ion modes. (B) Heatmaps of differential metabolites between Area A and Area B with VIP values > 1 and T-test p-values < 0.05 under negative and positive ion modes. (C) Volcano plots of differential metabolites between Area A and Area C under negative and positive ion modes. (D) Heatmaps of differential metabolites between Area A and Area C with VIP values > 1 and T-test p-values < 0.05 under negative and positive ion modes. (neg: negative ion modes; pos: positive ion modes; A: the liver tissue from normal mice (Area A); B: the liver area outside the granulomas in mice of schistosomiasis (Area B); C: the granuloma region in mice of schistosomiasis (Area C))
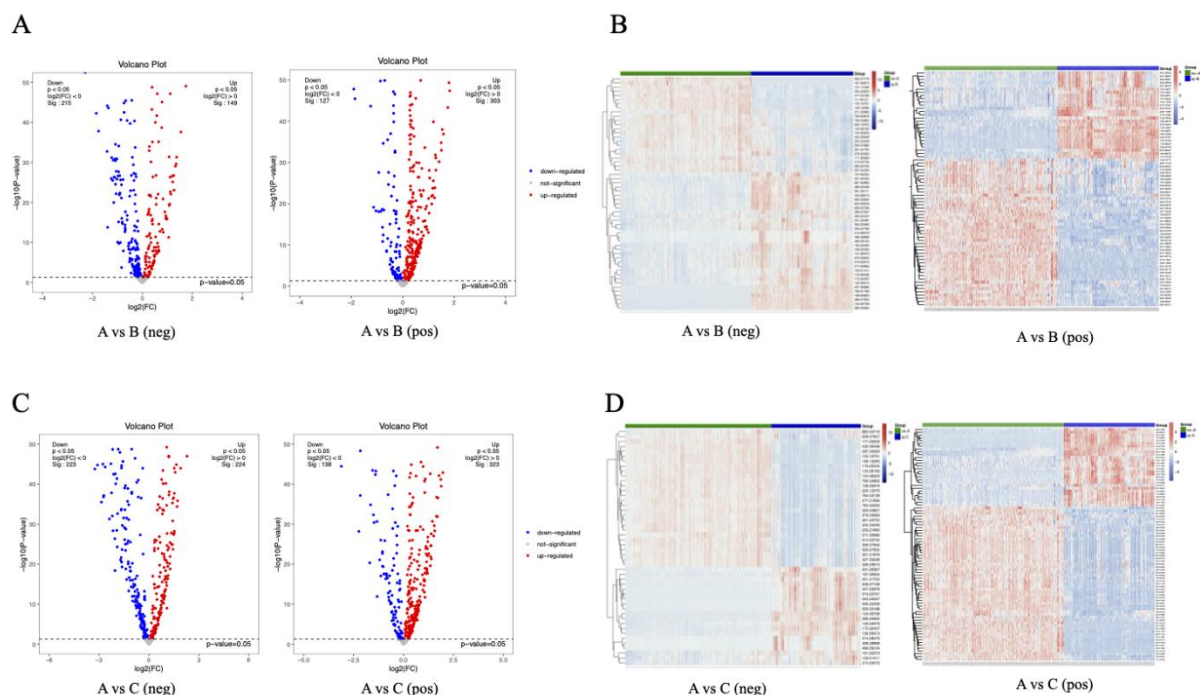
Figure 3. Functional enrichment analysis of differential metabolites. (A) Bubble plot of KEGG functional enrichment for differential metabolites with VIP values > 1 and T-test p-values < 0.05 between Area A and Area B. (B) Bubble plot of KEGG functional enrichment for differential metabolites with VIP values > 1 and T-test p-values < 0.05 between Area A and Area C. (A: the liver tissue from normal mice (Area A); B: the liver area outside the granulomas in mice of schistosomiasis (Area B); C: the granuloma region in mice of schistosomiasis (Area C))
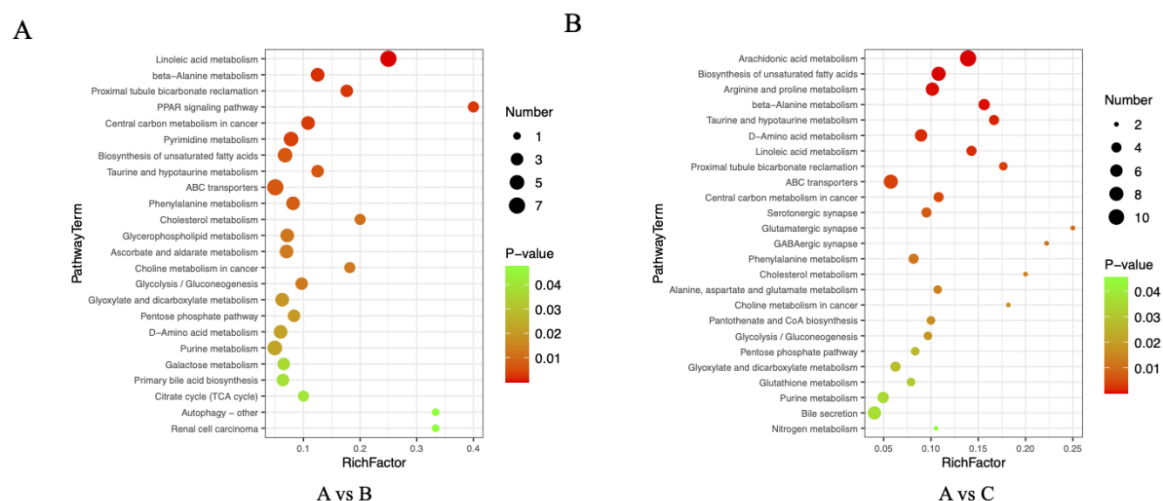
Figure 4. *In situ* distribution of unsaturated fatty acids in the liver of schistosomiasis. The spatial distribution of differential metabolites including unsaturated fatty acids FA (18:1), FA (18:2), FA (18:3), FA (20:1), FA (20:3), FA (20:4), FA (20:5), FA (22:4), and FA (22:6) in the livers of normal mice and mice with schistosomiasis. (NC: normal control mouse; SJ: *S. japonicum*-infected mice; neg: negative ion modes; pos: positive ion modes; FA: fatty acid)
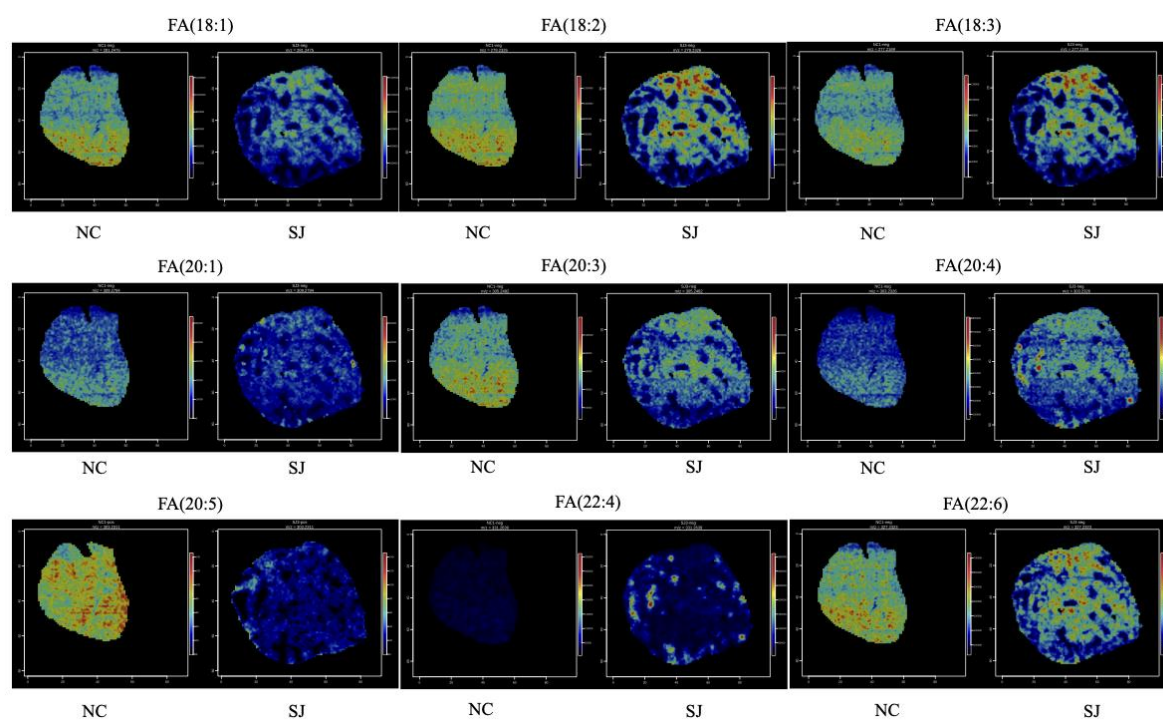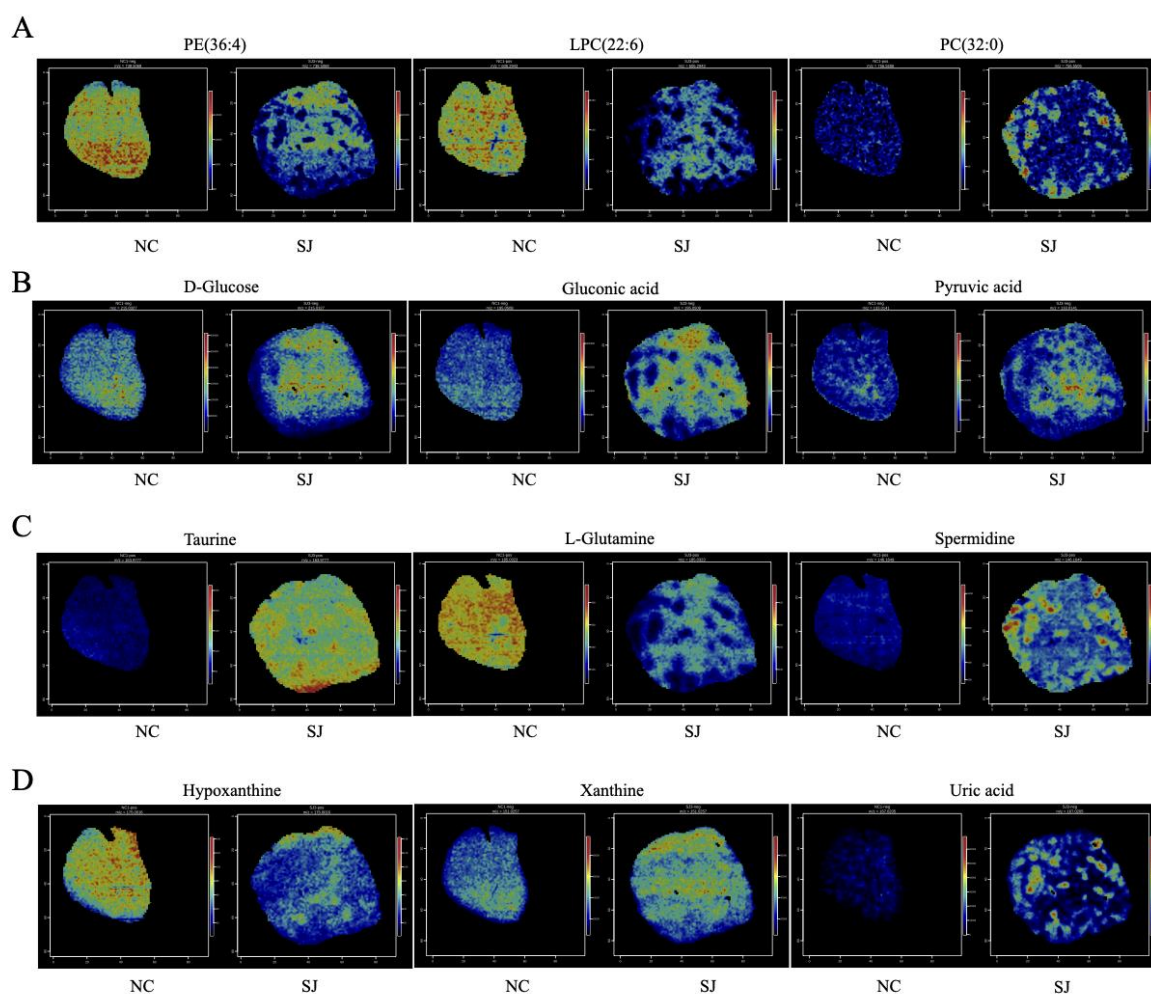
Figure 5. *In situ* distribution of crucial differential metabolites in the liver of schistosomiasis. (A) The spatial distribution of PE (36:4), LPC (22:6), and PC (32:0) in the livers of normal mice and mice with schistosomiasis. (B) The spatial distribution of D-glucose, gluconic acid, and pyruvic acid in the livers of normal mice and mice with schistosomiasis. (C) The spatial distribution of taurine, L-glutamine, and spermidine in the livers of normal mice and mice with schistosomiasis. (D) The spatial distribution of hypoxanthine, xanthine, and uric acid in the livers of normal mice and mice with schistosomiasis. (NC: normal control mouse; SJ: *S. japonicum*-infected mice; neg: negative ion modes; pos: positive ion modes; PE: phosphatidylethanolamine; LPC: lysophosphatidylcholine; PC: phosphatidylcholine)

Graphical Abstract: